Available online at www.sciencedirect.com
SCIENCE DIRECT
Polymer 47 (2006) 3540–3547
polymer
www.elsevier.com/locate/polymer

Lamellar crystalline structure of hard elastic HDPE films and its influence on microporous membrane formation

Sang-Young Lee [a,*], Soon-Yong Park [b], Heon-Sik Song [b]

[a] Batteries R&D, LG Chem, 104-1, Moonji-dong, Yusong-gu, Daejon 305-380, South Korea
[b] Information and Electronic Materials R&D, LG Chem, 104-1, Moonji-dong, Yusong-gu, Daejon 305-380, South Korea

Received 29 November 2005; received in revised form 4 March 2006; accepted 18 March 2006

Abstract

The development of hard elastic high-density polyethylene (HDPE) precursor films and its influence on the microporous membrane formation have been investigated. As a first step, the HDPE precursor films with 'row-nucleated lamellar crystalline' structure were prepared by applying elongation stress to the HDPE melt during T-die cast film extrusion and subsequently annealing the extruded films. This unusual crystalline structure was analyzed in terms of lamellar crystalline orientation, long-period lamellar spacing, crystallite size, and degree of crystallinity. The processing (melt extension and annealing temperature)-structure (lamellar crystalline structure)–property (hard elasticity) relationship of HDPE precursor films was also investigated. The uniaxial stretching of hard elastic HDPE precursor films induces the bending of crystalline lamellae, which leads to the formation of micropores between them. The observation of morphology and air permeability for the HDPE microporous membranes have revealed that the well-developed porous structures characterized by superior air permeability were established preferably from the precursor films prepared by the high stress levels and the high annealing temperatures. Finally, the relationship between the hard elasticity of HDPE precursor films and the air permeability of corresponding microporous membranes was discussed.

Keywords: HDPE; Lamellar crystalline; Microporous membrane

1. Introduction

Over the past years, 'hard elastic' polymers have attracted much attention due to their possible applications to precursor films for preparing microporous membranes [1–21]. They are characterized by high modulus of elasticity, reversible deformation, energetic retractive force, and constant cross-sectional area during deformation. These unusual properties are believed to be due to their 'row-nucleated lamellar crystalline' structures that comprise rows of crystalline lamellae arranged preferentially normal to draw direction and connected by tie chains. The lamellar crystalline structure can be formed when polymers having high degree of crystallinity are melt-extruded with experiencing elongation stress and then recrystallized, which is called as 'stress-induced crystallization' [1–9]. This type of hard elastic behavior has been reported in polypropylene [1,4,10–16,19], polymethylbutene [2], polyethylene [3,5–13,20,21], polystyrene [17], nylon 66 [18]. When the hard elastic polymer is annealed and extended in the orientation direction, the portions of crystalline lamellae that are not connected by tie chains move apart, which leads to the bending of crystalline lamellae and the formation of micropores between them [10–13,18–21].

Therefore, in order to have a comprehensive understanding of the microporous membrane formation, a more quantitative analysis on the processing-structure–property relationship of the hard elastic precursor films as well as the microporous membranes is needed. In this study, as a first step, the effects of processing variables such as screw rpm and take-up speed (during T-die cast film extrusion) and annealing temperature on the development of lamellar crystalline structures in the HDPE precursor films were examined. The row-nucleated lamellar crystalline structures were analyzed in terms of lamellar crystalline orientation, long-period lamellar spacing, crystallite size, and degree of crystallinity. The relationship between the lamellar crystalline structures of HDPE precursor films and their hard elastic properties was also investigated. Following this fundamental analysis on the lamellar crystalline structures and the hard elasticity of HDPE precursor films, their influences on the morphology development and the air

* Corresponding author. Tel.: +82 42 866 5851; fax: +82 42 863 2934.
E-mail address: syleeq@lgchem.com (S.-Y. Lee).

0032-3861/$ - see front matter © 2006 Elsevier Ltd. All rights reserved.
doi:10.1016/j.polymer.2006.03.070

permeability of HDPE microporous membranes were discussed.

2. Experimental

2.1. Preparation of HDPE precursor films

A commercial grade of HDPE resin (melt index (g/10 min, 190 °C, 2160 g) = 0.35) was used. The HDPE resin was melt-extruded through a T-die under controlled processing conditions. During the T-die extrusion, the uniaxial (machine direction, MD) stretching was applied to the HDPE melt, which results in the oriented crystalline structures [22–24]. The melt flow rate at die exit and the degree of melt extension were varied by controlling either the velocity of melt outflow from die exit or the rotation velocity of take-up roll (chill roll). The degree of melt extension was described as draw-down-ratio, DDR = V_2/V_1, where V_1 is the velocity of melt outflow from die exit, and V_2 is the linear velocity of rotation of take-up roll. Another factor influencing the structural rearrangement of HDPE precursor films, i.e. annealing temperature is controlled by annealing the extruded films for 1 h at various temperatures (from 95 to 125 °C) in a hot oven. The detailed processing variables for preparation of the hard elastic HDPE precursor films were summarized in Table 1. The HDPE microporous membranes were prepared by uniaxial (machine direction, MD) stretching of the annealed (125 °C/1 h) precursor films. In case that the HDPE precursor films were subjected to the uniaxial stretching without pre-treatment of annealing, it was hardly possible to obtain microporous membranes with appreciable values of air permeability. The annealed films were stretched to 50% of initial length at 25 °C and subsequently they were further extended to 150% of initial length at 125 °C. Finally, the stretched films passed through the thermo-fixation at 125 °C for 1 h. The whole stretching process was conducted by using a lab-stretching machine (Toyoseiki Ltd, Japan).

Table 1
Processing variables for preparing HDPE precursor films

Sample no.	Screw RPM	V_1 (m/min)	Take-up speed (V_2) (m/min)	DDR	Annealing temperature (°C)
V_1-1	5	0.193	10	51.9	None
V_1-2	10	0.316	16	50.6	None
V_1-3	20	0.600	29	48.3	None
V_1-4	30	0.847	42	49.6	None
DDR-1	10	0.316	5	15.8	None
DDR-2	10	0.316	10	31.6	None
DDR-3	10	0.316	16	50.6	None
DDR-4	10	0.316	22	69.6	None
Anneal-1	10	0.316	16	50.6	None
Anneal-2	10	0.316	16	50.6	95
Anneal-3	10	0.316	16	50.6	110
Anneal-4	10	0.316	16	50.6	125

2.2. Analysis

The birefringence (BR) of HDPE precursor films was measured on a polarizing microscope using N&K analyzer1200 (N&K Technology Inc., USA) with varying orders of retardation. The melting peak temperature and the heat of fusion of HDPE precursor films were recorded from the DuPont Thermal Analyst 2000 model differential scanning calorimeter (DSC) at a heating rate of 10 °C/min. The lamellar thickness and its distribution were calculated by applying the DSC experimental results to the 'Thomson' equation [25,26]. The elastic recovery (ER) of HDPE precursor films was determined from a stress–strain curve during cyclic loading of samples by using a Zwick 1100 tensile tester (Zwick Ltd, Germany), which can be used as an index for representing the structural arrangement and the hard elasticity of lamellar crystalline structure. The initial length of test samples was 50 mm, the strain rate was 100%/min, and the maximum tensile strain was 100%. After the sample is extended to 100% strain, jaws of the apparatus are reversed at the same speed until the distance between them becomes the same as at the start of the test, i.e. the original gauge length. The jaws are again immediately reversed and are stopped as soon as the stress begins to increase from zero point. The elastic recovery is then calculated in Eq. (1) [6,7,10–13];

$$\text{Elastic recovery (ER, \%)} = 100\frac{\{(\text{total length when extended}) - (\text{length recovered after having been subjected to stretching})\}}{\{(\text{total length when extended}) - (\text{length before being subject to the stretching})\}} \quad (1)$$

The lamellar crystalline morphology of the HDPE precursor films and their corresponding microporous membranes was observed from a JSM-6340F (JEOL Ltd, Japan) field emission scanning electron microscopy (FE-SEM). The air permeability of the HDPE microporous membranes was measured from 'gurley type densometer' (Toyoseiki Ltd, Japan), following the procedure described in JIS P8117, and was given by gurley value (s). The gurley value that is widely used in characterizing air permeability of microporous membranes, is determined to measure the elapsed time of air to pass through a determined volume (here, 100 cm^3) under a given pressure (here, 20 kgf/cm^2) [10–13], where low gurley value corresponds to high air permeability.

3. Results and discussion

3.1. Structure and properties of lamellar crystalline HDPE precursor films

The crystalline structures and the properties of HDPE precursor films were investigated as a function of melt flow rate at die exit (V_1), degree of melt extension (DDR), and annealing

temperature. Fig. 1 shows that the birefringence (BR) of HDPE precursor films tends to increase with V_1, DDR, and annealing temperature. The BR measurement is known to be an effective way for characterizing the overall orientation of hard elastic materials [8,20]. The high BR is possibly attributed to the lamellar crystalline and molecular orientation. The influence of V_1, DDR, and annealing temperature on the BR was quantitatively examined. In Fig. 1, from the slopes, $\Delta(\mathrm{BR}-V_1)=0.005$, $\Delta(\mathrm{BR}-\mathrm{DDR})=0.025$, and $\Delta(\mathrm{BR}-T_{\mathrm{annealing}})=0.018$ were, respectively, obtained. This presents that the DDR is most effective in increasing the overall orientation of HDPE chains.

The apparent lamellar thickness of HDPE precursor films was obtained by measuring the melting peak temperature ($T_{\mathrm{m,peak}}$) and the heat of fusion (ΔH_{m}) from the DSC results. It is suggested that at a given temperature for a sample of molten polymer, the rate of heat consumption is proportional to the fraction of crystalline lamellae. The apparent lamellar thickness can be calculated by 'Thomson' equation [25,26], $T_{\mathrm{m}} = T_{\mathrm{m}}^0(1-2\sigma_{\mathrm{e}}/\Delta H_{\mathrm{m}}^0 \ell)$, where T_{m} is the observed melting point of lamellae of thickness ℓ, T_{m}^0 is the equilibrium melting point of an infinite crystal ($T_{\mathrm{m}}^0 = 415$ K for polyethylene [25]), σ_{e} is the surface free energy of the basal plane ($\sigma_{\mathrm{e}}=6.09\times10^{-2}$ J/m^2 for polyethylene [25]), ΔH_{m}^0 is the enthalpy of fusion per unit volume ($\Delta H_{\mathrm{m}}^0 = 2.88\times10^{-8}$ J/m^2 for polyethylene [25]), and ℓ is the lamellar thickness. The calculated lamellar thickness is summarized in Fig. 2, which shows that the apparent lamellar thickness is influenced noticeably by the annealing temperature than other processing variables.

To have a more detailed understanding of the effect of annealing process on the crystalline structure, the changes of T_{m} and ΔH_{m} are investigated as a function of the annealing temperature. Fig. 3(a) exhibits that the T_{m} seems to be little affected by the change of annealing temperature. However, the ΔH_{m} was observed to increase from 190.9 J/g for no annealed sample to 222.0 J/g for 125 °C—annealed sample. This result reflects that the annealing temperature has larger influence on the overall degree of crystallinity (reflected by ΔH_{m}) rather than on the perfectness of crystal (reflected by T_{m}). The lamellar thickness distribution was calculated by using the 'Thomson' equation. Fig. 3(b) exhibits the distribution of lamellar thickness annealed at various temperatures. As the annealing temperature increases, the lamellar thickness tends to be larger and its distribution becomes broad. It is possibly expected that under high annealing temperature, involving the segments of loose tie chains into the crystallites is probably induced, which may result in the increase of lamellae thickness (i.e. long-period lamellar spacing) and the increase in the overall degree of crystallinity. Chen et al. [20] suggested that by employing small angle X-ray scattering (SAXS) analysis, long period lamellar spacing increases with annealing temperature up to melting peak temperature.

The elastic recovery (ER) can be used as an indicator for characterizing the elastic deformation properties of lamellar crystalline structures [6,7,10–13]. An ideal model of hard elastic material presents its structure as a combination of stacks of lamellae arranged perpendicular to melt flow direction

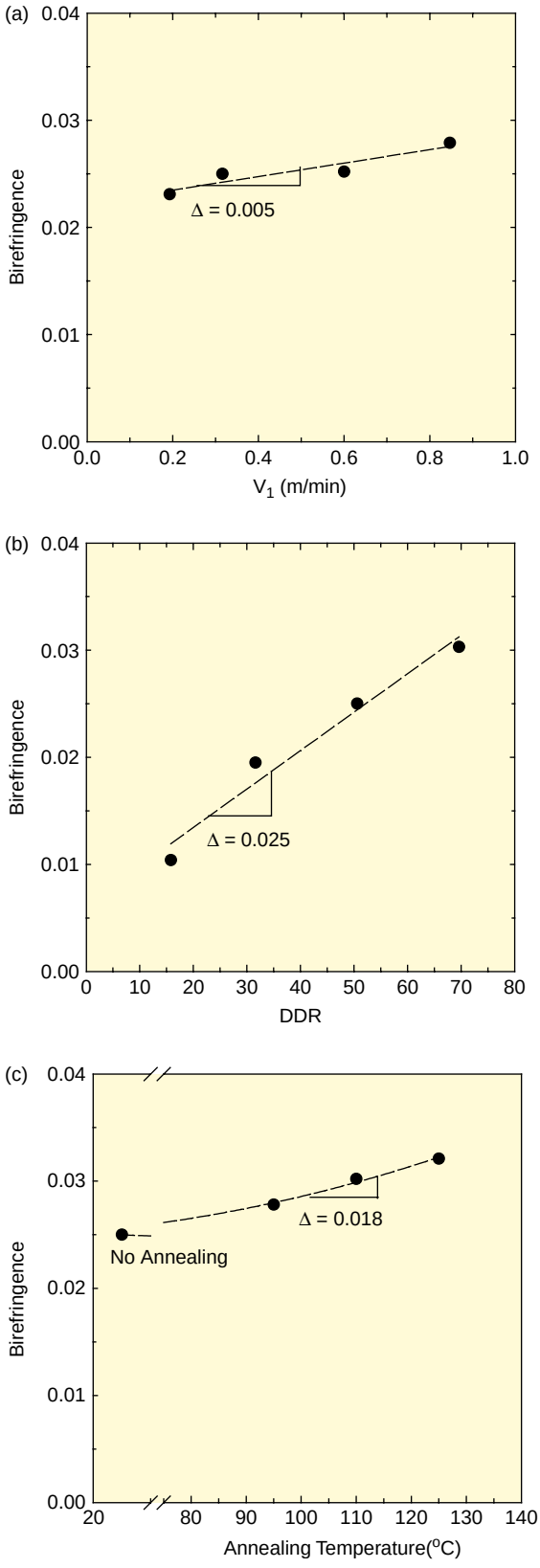

Fig. 1. Effects of melt flow rate at die exit (V_1), degree of melt extension (DDR), and annealing temperature (T_{ann}) on birefringence (BR) of HDPE precursor films. (a) Birefringence (BR) vs. melt flow rate at die exit (V_1). (b) Birefringence (BR) vs. degree of melt extension (DDR). (c) Birefringence (BR) vs. annealing temperature (T_{ann}).

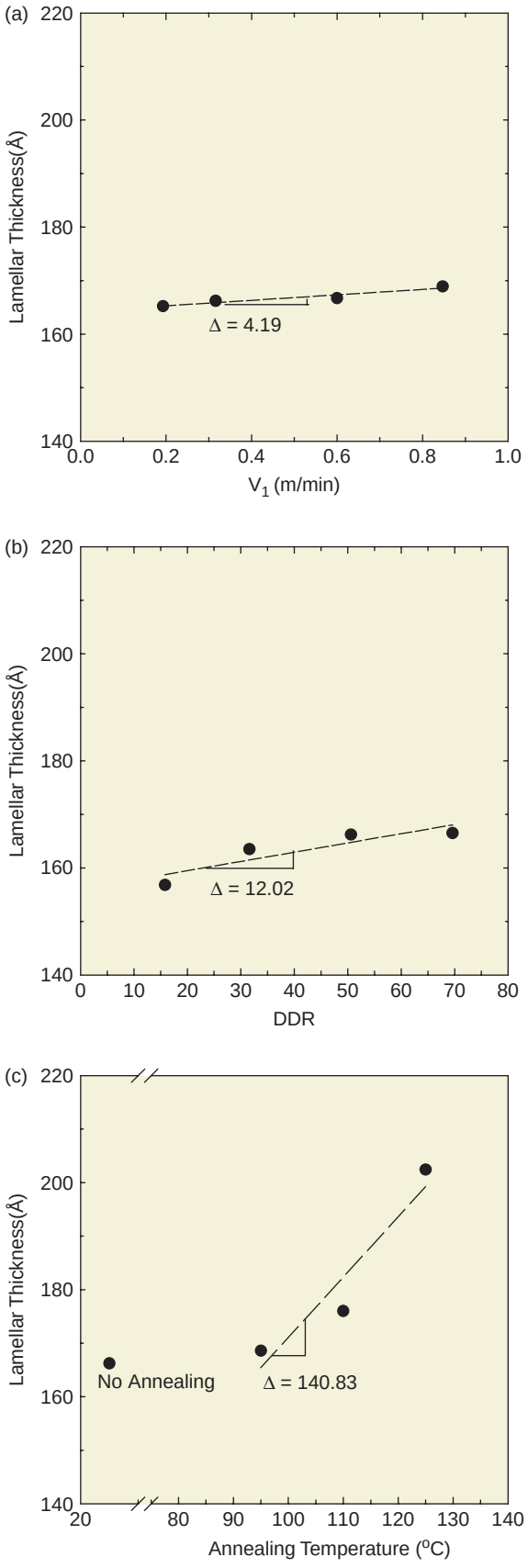

Fig. 2. Effects of melt flow rate at the die exit (V_1), degree of melt extension (DDR), and annealing temperature (T_{ann}) on apparent lamellar thickness (ℓ_{app}) of HDPE precursor films. (a) Apparent lamellar thickness (ℓ_{app}) vs. melt flow rate at die exit (V_1). (b) Apparent lamellar thickness (ℓ_{app}) vs. degree of melt extension (DDR). (c) Apparent lamellar thickness (ℓ_{app}) vs. annealing temperature (T_{ann}).

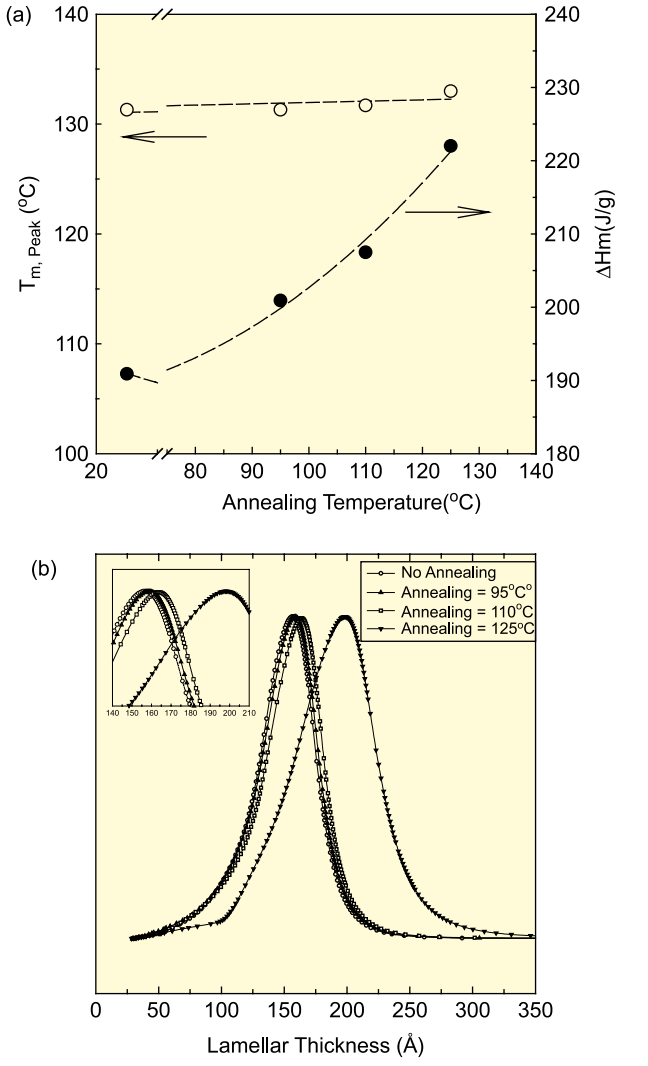

Fig. 3. Effects of annealing temperature on melting peak temperature and lamellar thickness distribution of HDPE precursor films. (a) Melting peak temperature ($T_{m,peak}$) vs. annealing temperature (T_{ann}). (b) Lamellar thickness distribution (ℓ) as a function of annealing temperature (T_{ann}).

[1–5,14–16]. In Fig. 4, it is shown that the ER becomes larger as V_1, DDR, and annealing temperature increases. Considering the slope of ER against V_1 and DDR, it is also observed that the ER appears to be more dependent on the DDR rather than the V_1, which is consistent with our previous results on the birefringence. Besides the stress conditions, the annealing temperature is also found to largely influence the ER (Fig. 4(c)). Rosova et al. [7] suggested that as the annealing temperature increases, the length of polymer chain folds starts to increase and the chain segments in the amorphous region are drawn into the crystallites, yielding the narrower length distribution of tie chains and the larger number of stretched tie chains. Within interlamellar regions containing a high concentration of stretched tie chains, these tie chains remain

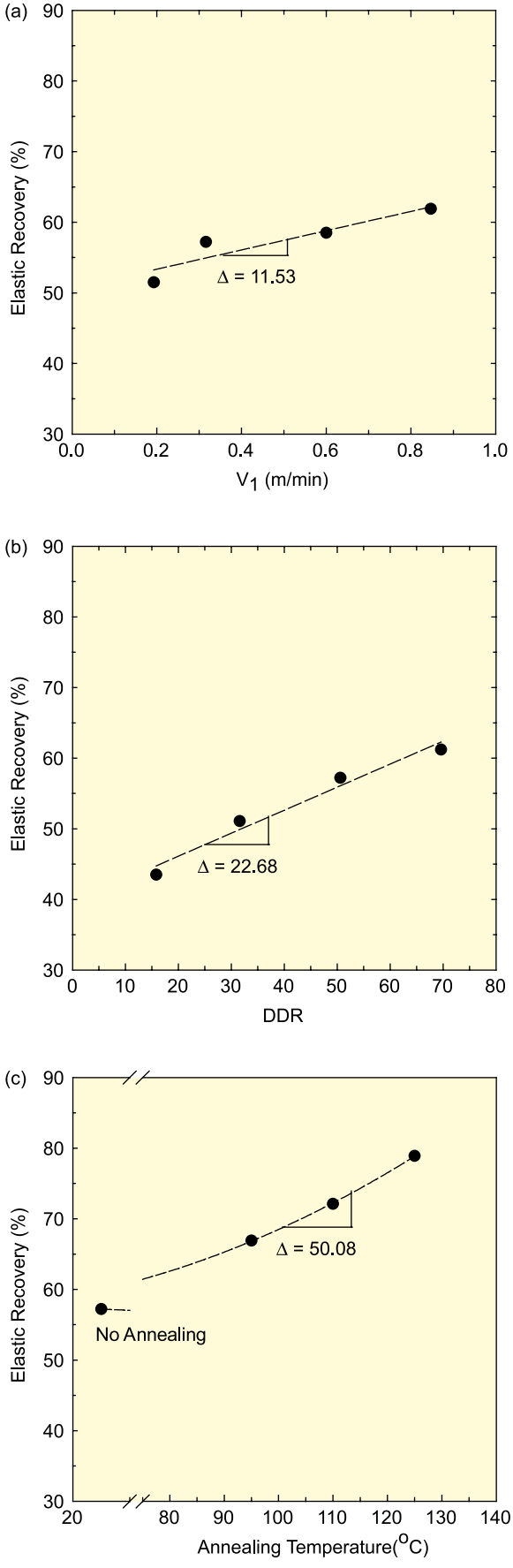

Fig. 4. Effects of melt flow rate at die exit (V_1), degree of melt extension (DDR), and annealing temperature (T_{ann}) on elastic recovery (ER) of HDPE precursor films. (a) Elastic recovery (ER) vs. melt flow rate at die exit (V_1). (b) Elastic recovery (ER) vs. degree of melt extension (DDR). (c) Elastic recovery (ER) vs. annealing temperature (T_{ann}).

intact and function as cross-links, which may be responsible for the elastic character of lamellar bending.

This elastic recoverable nature of HDPE precursor films is also evidently observed from the FE-SEM images that indicate the anisotropic lamellar crystalline structures (Fig. 5). It is seen that when the high elongation stress was applied, the crystalline lamellae tilted toward preferential alignment with respect to stretching direction and the lamellar twisting hardly occurred, resulting in a well-developed stacked lamellar structure (Fig. 5(a)–(d)). Meanwhile, the annealing temperature was observed to affect the lamellar thickness rather than the alignment direction of the crystalline structure (Fig. 5(e) and (f)), which is consistent with the previous DSC results (Fig. 3) on the lamellar crystalline structures.

By summarizing the results of this study, we can figure out the processing (DDR and annealing temperature)-structure (lamellar crystalline alignment)–property (elastic recovery) relationship. The preferential lamellar crystalline alignment with respect to the stress direction (governed mainly by the DDR) and the larger long-period lamellar spacing, i.e. the larger number of stretched tie chains (governed mainly by the annealing temperature) are observed to have a significant influence on the increase of the elastic recovery (ER).

3.2. Morphology and air permeability of HDPE microporous membranes

The morphology and the air permeability of HDPE microporous membranes were examined and their relationship with the hard elasticity of HDPE precursor films was discussed. The HDPE microporous membranes were prepared by uniaxial stretching of the annealed precursor films and subsequently through thermo-fixation.

Fig. 6 presents the morphology of HDPE microporous membranes as a function of processing variables such as melt flow rate at the die exit (V_1), degree of melt extension (DDR), and annealing temperature. The micropores between the deformed lamellar crystalline appear to be tightened by stressed tie molecular chains and show a slit-like shape in a pocket fashion. It is also seen in Fig. 6 that the well-developed porous structures with large number of pores and relatively uniform pore size distribution were formed preferably at the high stress levels (especially, high DDR) and the high annealing temperatures, which reflects that these unique microporous structures highly depend on the hard elastic properties of HDPE precursor films.

As a next step, the air permeability of HDPE membranes is investigated and correlated with the microporous structures. From a practical point of view, air permeability can be expressed by gurley value [10–13], where low gurley value corresponds to high air permeability. It is shown in Fig. 7 that

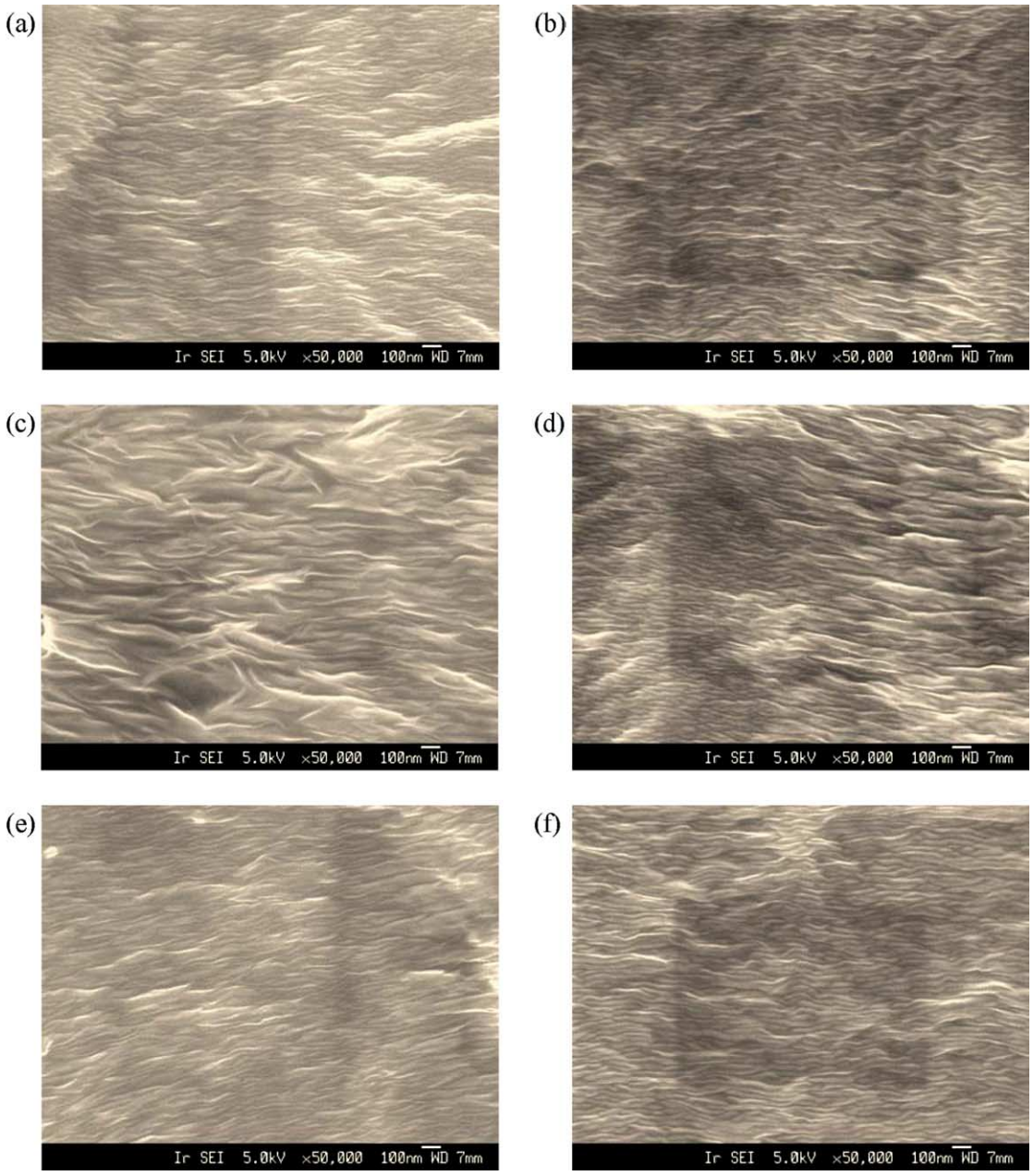

Fig. 5. FE-SEM photomicrographs of HDPE films as a function of melt flow rate at die exit (V_1), degree of melt extension (DDR), and annealing temperature (T_{ann}). (a) V_1-1 (=0.193 m/min). (b) V_1-4 (=0.847 m/min). (c) DDR-1 (=15.8). (d) DDR-4 (=69.6). (e) Anneal-1 (=none). (f) Anneal-4 (=125 °C).

the increase of V_1, DDR, and annealing temperature contributes to the decrease of gurley value for HDPE microporous membranes. Especially, the effects of DDR and annealing temperature on the gurley value appear to be more noticeable, which is consistent with the previous morphological observation.

Finally, the relationship between the HDPE microporous membranes and the corresponding precursor films is discussed. In Fig. 8, the gurley values of HDPE microporous membranes are plotted as a function of the elastic recovery of precursor films. It is shown that the gurley values tend to be inversely proportional to the elastic recovery, which implies that the HDPE precursor films with the higher elastic recovery could contribute to the formation of well-developed HDPE microporous membranes with the low gurley values (i.e. high air permeability). The significance of this relationship is that it can be regarded as a kind of indicator for predicting the air permeability of HDPE microporous membranes just by measuring the elastic recovery of corresponding precursor films, without an effort for preparing the HDPE microporous membranes and measuring their air permeability.

4. Conclusion

This study has presented comprehensive information on the lamellar crystalline development in the HDPE precursor films

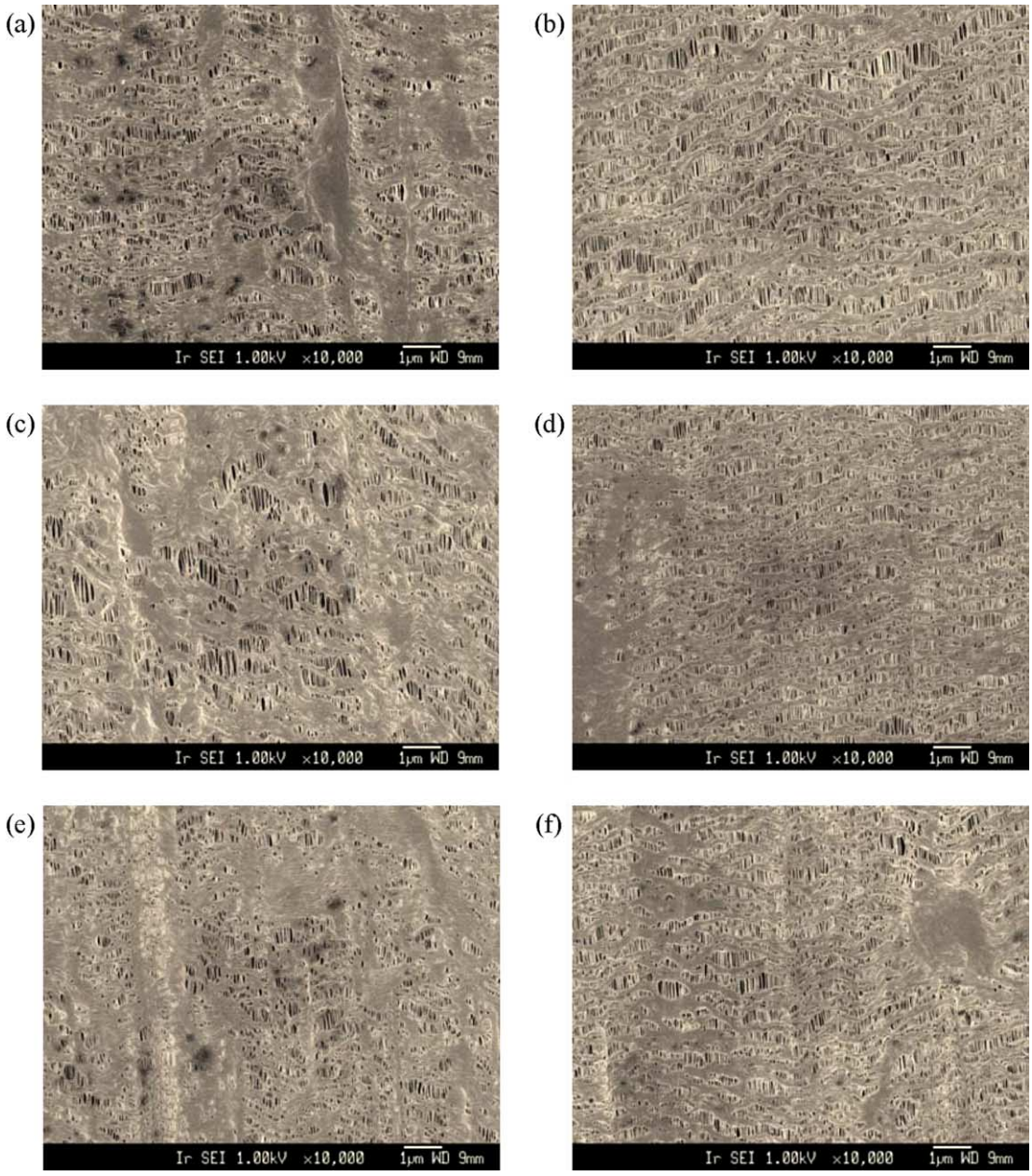

Fig. 6. FE-SEM photomicrographs of HDPE microporous membranes as a function of melt flow rate (V_1) at die exit and degree of melt extension (DDR) and annealing temperature (T_{ann}). (a) V_1-1 (=0.193 m/min). (b) V_1-4 (=0.847 m/min). (c) DDR-1 (=15.8). (d) DDR-4 (=69.6). (e) Anneal-2 (=95 °C). (f) Anneal-4 (=125 °C).

and its influence on the corresponding microporous membrane formation. The row-nucleated lamellar crystalline structures of HDPE precursor films were quantitatively analyzed in terms of the lamellar crystalline orientation, the long-period lamellar spacing, the crystallite size, and the crystallinity. The relationship between the lamellar crystalline structures of precursor films and their hard elastic properties was also investigated, which reveals that the highly oriented lamellar crystalline structure (influenced by the DDR) and the larger number of stretched tie chains (influenced by the annealing temperature) contribute to the high modulus of elasticity and the reversible deformation of precursor films. The examination of morphology and air permeability for the HDPE microporous membranes have presented that the well-developed porous structures with the high air permeability (i.e. low gurley value) were established preferably from the precursor films prepared by the high stress levels (especially, high DDR) as well as the high annealing temperatures. It indicates that these unique microporous structures highly depend on the hard elastic properties of precursor films. Finally, the relationship between the air permeability of HDPE microporous membranes and the elastic recovery of corresponding precursor films was investigated. It provides meaningful information that without an effort for preparing the HDPE microporous membranes,

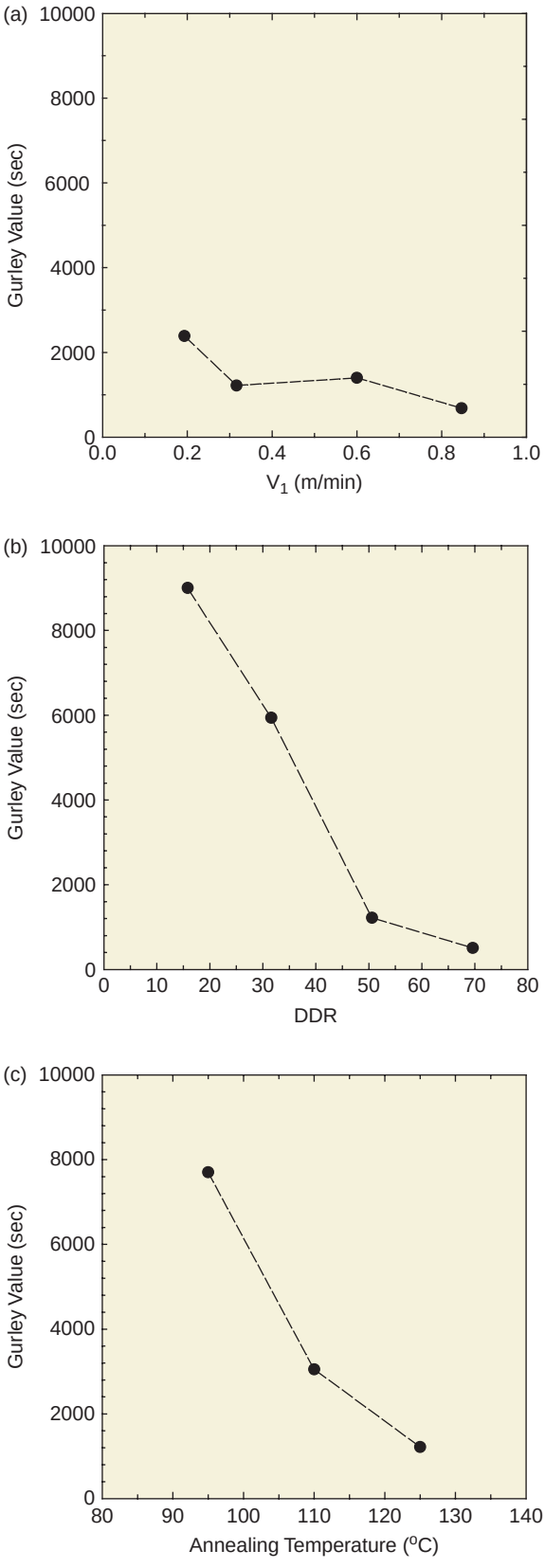

Fig. 7. Effects of melt flow rate (V_1) at die exit and degree of melt extension (DDR) and annealing temperature (T_{ann}) on gurley values of HDPE microporous membranes. Low gurley value corresponds to high air permeability. (a) Gurley value vs. melt flow rate at die exit (V_1). (b) Gurley value vs. degree of melt extension (DDR). (c) Gurley value vs. annealing temperature (T_{ann}).

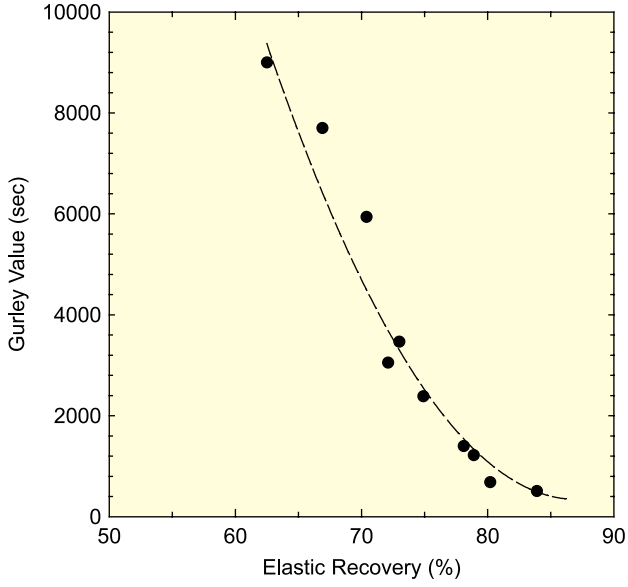

Fig. 8. Relationship between gurley value of HDPE microporous membranes and elastic recovery of HDPE precursor films.

the microporous structures and the air permeability of the membranes could be predicted from this relationship just by measuring the elastic recovery of the precursor films.

References

[1] Quynn RG, Brody H. J Macromol Sci Phys 1970;B4:953.
[2] Quynn RG, Sprague BS. J Polym Sci 1970;A-2:1971.
[3] Sprague S. J Macromol Sci 1973;B8:157.
[4] Cannon SL, Mckenna GB, Statton WO. J Polym Sci, Macromol Rev 1976;11:209.
[5] Tagawa T, Ogura K. J Polym Sci, Polym Phys Ed 1980;18:971.
[6] Karpov EA, Lavrent VK, Rosova EY, Elyashevich GK. Polym Sci, Ser A 1995;37:1247.
[7] Rosova EY, Karpov EA, Lavrentiev VK, Elyashevich GK. PPS-12 Annual Meeting 1996;1:297.
[8] Yu T, Wilkes GL. Polymer 1996;37:4675.
[9] Johnson MB, Yu TH, Wilkes GL. SPE ANTEC'99 1999:2261.
[10] Druin ML, Loft JT, Plovan SG. US Patent 1972:3679538.
[11] Taskier H. US Patent 1982:4359510.
[12] Kamei E, Ashitaka H, Takahashi T. US Patent 1992:5173235.
[13] Kurauchi H, Akazawa T, Kawabata A. European Patent 1995:0 682 376 A1.
[14] Wool RP. J Polym Sci, Polym Phys Ed 1976;14:603.
[15] Chou CJ, Hiltner A, Baer E. Polymer 1986;27:369.
[16] Hild S, Gutmannsbauer W, Luthi R, Fuhrmann J, Guntherodt HJ. J Polym Sci, Polym Phys Ed 1996;34:1953.
[17] Gu F, Bu H, Zhang Z. Macromolecules 2000;33:5490.
[18] Noether HD. Polym Eng Sci 1979;19:427.
[19] Sarada T, Sawyer LC, Ostler MI. J Membr Sci 1983;15:97.
[20] Chen RT, Saw CK, Jamieson MG, Aversa TR, Callahn RW. J Appl Polym Sci 1994;53:471.
[21] Elyashevich GK, Rosova EY, Karpov EA, Kudasheva OV. PPS-12 Annual Meeting 1996;1:297.
[22] Duffo P, Monasse B, Haudin M. Int Polym Process 1990;5:272.
[23] Degroot JA, Doughty AT, Stewart KB, Patel RM. J Appl Polym Sci 1994; 52:365.
[24] Iyengar VR, Co A. Chem Eng Sci 1996;51:1417.
[25] Hoffman JD. Treatise on solid state chemistry, vol. 1. NY, USA: Plenum Press; 1976.
[26] Wlochowicz A, Eder M. Polymer 1984;25:1268.